DIAL
Digital access to libraries

"Characterization of patient-derived tumor xenograft models of endometrial cancer for preclinical evaluation of targeted therapies"

Depreeuw, Jeroen ; Hermans, Els ; Schrauwen, Stefanie ; Annibali, Daniela ; Coenegrachts, Lieve ; Thomas, Debby ; Luyckx, Mathieu ; Gutierrez-Roelens, Ilse ; Debruyne, David ; Konings, Katrien ; Moerman, Philippe ; Vergote, Ignace ; Lambrechts, Diether ; Amant, Frédéric

Abstract

Objective Endometrial carcinoma (EC) is the sixth most common cancer in women and therapies are limited for advanced and recurrent disease. Patient-derived tumor xenograft (PDTX) models are becoming popular tools in translational research because of their histological and genetic similarity to the original tumors and the ability to predict therapeutic response to treatments. Here, we established and characterized a panel of 24 EC PDTX models which includes the major histological and genetic subtypes observed in patients. Methods Fresh tumor tissues collected from primary, metastatic and recurrent type I and type II EC patients were engrafted in immunocompromised mice. Histology, vimentin, and cytokeratin expression were evaluated, together with Microsatellite instability (MSI), mutation profiling by Whole Exome Sequencing and copy number profiling by Whole Genome Low Coverage Sequencing. The efficacy of both PI3K and MEK inhibitors was evaluated in a model of endometrioid carcinoma h...

Document type : *Article de périodique (Journal article)*

Référence bibliographique

Depreeuw, Jeroen ; Hermans, Els ; Schrauwen, Stefanie ; Annibali, Daniela ; Coenegrachts, Lieve ; et. al. *Characterization of patient-derived tumor xenograft models of endometrial cancer for preclinical evaluation of targeted therapies.* In: *Gynecologic Oncology*, Vol. 139, no. 1, p. 118-126 (2015)

DOI : 10.1016/j.ygyno.2015.07.104

Available at:
http://hdl.handle.net/2078.1/168635

[Downloaded 2019/04/19 at 02:06:35]

Gynecologic Oncology 139 (2015) 118–126

Contents lists available at ScienceDirect

Gynecologic Oncology

journal homepage: www.elsevier.com/locate/ygyno

Characterization of patient-derived tumor xenograft models of endometrial cancer for preclinical evaluation of targeted therapies

Jeroen Depreeuw [a,b,c,1], Els Hermans [a,1], Stefanie Schrauwen [a,1], Daniela Annibali [a], Lieve Coenegrachts [a], Debby Thomas [a], Mathieu Luyckx [d], Ilse Gutierrez-Roelens [e], David Debruyne [f], Katrien Konings [a], Philippe Moerman [g], Ignace Vergote [a], Diether Lambrechts [b,c], Frédéric Amant [a,h,*]

[a] KU Leuven — University of Leuven, University Hospitals Leuven, Division of Gynecologic Oncology, Department of Obstetrics and Gynecology, B-3000 Leuven, Belgium
[b] KU Leuven, Department of Oncology, Laboratory for Translational Genetics, B-3000 Leuven, Belgium
[c] VIB, Vesalius Research Center (VRC), B-3000 Leuven, Belgium
[d] UCL — Université Catholique de Louvain, University Hospitals Saint-Luc, Division of Surgical Gynecology, Department of Surgery, B-1200 Brussel, Belgium
[e] UCL — Université Catholique de Louvain, University Hospitals Saint-Luc, King Albert II Institute Biolibrary, B-1200 Brussels, Belgium
[f] Department of Gynecology, AZ Groeninge Hospital, B-8500 Kortrijk, Belgium
[g] KU Leuven — University of Leuven, University Hospitals Leuven, Division of Translational Cell & Tissue Research, Department of Imaging and Pathology, B-3000 Leuven, Belgium
[h] Gynaecological Oncology, Netherlands Cancer Institute-Antoni Van Leeuwenhoek, Amsterdam, The Netherlands

HIGHLIGHTS

- Patient-derived tumor xenografts (PDTXs) can be established from endometrial cancer.
- Endometrial cancer PDTXs maintain the general features of the human tumor.
- Such models can be used as preclinical tools to study therapy response.

GRAPHICAL ABSTRACT

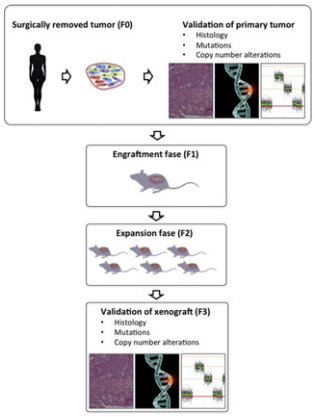

General overview of the establishment of endometrial PDTX models. Primary tumor tissue (F0) was surgically removed and implanted in mice. In parallel, remaining tissue was fresh-frozen and formalin-fixed for histological and genetic analysis. After engraftment (F1), tumor tissue was implanted in new mice for expansion (F2). Tumors were further transplanted in F3 generation for histological and genetic validation and compared with the primary tumor.

* Corresponding author at: KU Leuven — University of Leuven, University Hospitals Leuven, Division of Gynecologic Oncology, Department of Obstetrics and Gynecology, UZ Herestraat 49 — bus 7003, 3000 Leuven, Belgium.
E-mail addresses: Jeroen.Depreeuw@vib-kuleuven.be (J. Depreeuw), Els.Hermans@uzleuven.be (E. Hermans), Stefanie.Schrauwen@med.kuleuven.be (S. Schrauwen), Daniela.Annibali@kuleuven.be (D. Annibali), coenegrachtslieve@hotmail.com (L. Coenegrachts), debby.thomas@med.kuleuven.be (D. Thomas), mathieu.luyckx@uclouvain.be (M. Luyckx), ilse.gutierrez@uclouvain.be (I. Gutierrez-Roelens), David.Debruyne@azgroeninge.be (D. Debruyne), kkonings@SCKCEN.be (K. Konings), Philippe.Moerman@uzleuven.be (P. Moerman), Ignace.Vergote@uzleuven.be (I. Vergote), Diether.Lambrechts@vib-kuleuven.be (D. Lambrechts), Frederic.Amant@uzleuven.be (F. Amant).
[1] shared first authorship.

http://dx.doi.org/10.1016/j.ygyno.2015.07.104
0090-8258/© 2015 Elsevier Inc. All rights reserved.

ARTICLE INFO

Article history:
Received 20 April 2015
Received in revised form 10 July 2015
Accepted 25 July 2015
Available online 29 July 2015

Keywords:
Endometrial cancer
Patient-derived tumor xenografts
Preclinical models
Targeted therapy

ABSTRACT

Objective. Endometrial carcinoma (EC) is the sixth most common cancer in women and therapies are limited for advanced and recurrent disease. Patient-derived tumor xenograft (PDTX) models are becoming popular tools in translational research because of their histological and genetic similarity to the original tumors and the ability to predict therapeutic response to treatments. Here, we established and characterized a panel of 24 EC PDTX models which includes the major histological and genetic subtypes observed in patients.

Methods. Fresh tumor tissues collected from primary, metastatic and recurrent type I and type II EC patients were engrafted in immunocompromised mice. Histology, vimentin, and cytokeratin expression were evaluated, together with Microsatellite instability (MSI), mutation profiling by Whole Exome Sequencing and copy number profiling by Whole Genome Low Coverage Sequencing. The efficacy of both PI3K and MEK inhibitors was evaluated in a model of endometrioid carcinoma harboring *PTEN*, *PIK3CA* and *KRAS* mutations.

Results. We observed good similarity between primary tumors and the corresponding xenografts, at histological and genetic level. Among the engrafted endometrioid models, we found a significant enrichment of MSI and *POLE* mutated tumors, compared to non-engrafted samples. Combination treatment with NVP-BEZ235 and AZD6244 showed the possibility to stabilize the tumor growth in one model originated from a patient who already received several lines of chemotherapy.

Conclusion. The established EC PDTX models, resembling the original human tumors, promise to be useful for preclinical evaluation of novel combination and targeted therapies in specific EC subgroups.

© 2015 Elsevier Inc. All rights reserved.

1. Introduction

Endometrial carcinoma (EC) is the most common gynecological malignancy in the Western World, and the number of new cases is expected to rise in the next 10 years [1]. ECs are traditionally classified into two main groups. Type I ECs, with endometrioid histology, represent 80% of the cases and count for 15–20% of recurrences. In contrast, type II tumors, consisting of serous or clear cell histology, are less common but account for more than 50% of recurrences [2]. Since treatment options for advanced, metastatic and recurrent disease are currently limited in efficacy, there is an urgent need for clinical implementation of novel therapeutic strategies.

The recent comprehensive molecular characterization from TCGA revealed that, based on integrated genomic analysis, ECs can be

Table 1
Overview of patient characteristics and engrafted patient-derived tumor xenograft models of endometrial cancer.

ID PDTX model	Histology	Primary/recurrence	Grade	FIGO	Before engraftment		After engraftment		Survival since diagnosis (months)	Time F0–F1 (months)
					Treatment	Response	Treatment	Response		
PDTX-EMC028	Endometrioid	Primary	1	I	No	NA	No	NA	>24	9
PDTX-EMC032	Endometrioid	Primary	1	I	No	NA	No	NA	12–24	8
PDTX-EMC044	Endometrioid	Primary	1	I	No	NA	Doc-Cyclo	Yes	12–24	3
PDTX-EMC015	Endometrioid	Primary	1	III	T-C	partial	No	NA	NA	3
PDTX-EMC001	Endometrioid	Primary	2	IV	No	NA	P-C	Yes	NA	5
PDTX-EMC034	Endometrioid	Recurrence (vagina)	2	NA	No	NA	No	NA	>24	4
PDTX-EMC016	Endometrioid	Primary	2	I	No	NA	No	NA	>24	1.5
PDTX-EMC049	Endometrioid	Primary	2	I	No	NA	No	NA	12–24	4.5
PDTX-EMC040	Endometrioid	Primary	3	I	No	NA	T-C	Yes	12–24	7
PDTX-EMC046	Endometrioid	Primary	3	III	No	NA	No	NA	NA	3
PDTX-EMC003	Endometrioid	Recurrence (vagina)	3	NA	D-Cis; H; Ixa;C	no	no	NA	> 24	3
PDTX-EMC056	Endometrioid with undifferentiated component	Primary	3	I	No	NA	No	NA	6–12	4
PDTX-EMC042	Mixed Endometrioid/ Clear cell	Primary	3	III	No	NA	No	NA	NA	4
PDTX-EMC039	Mixed Endometrioid/ Clear cell	Metastasis (peritoneum)	3	IV	No	NA	P-C	Yes	12–24	4.5
PDTX-EMC035	Mixed Serous/ Clear cell	Primary	3	III	No	NA	T-C	Yes	12–24	3
PDTX-EMC033	Serous	Primary	3	I	No	NA	No	NA	12–24	7
PDTX-EMC051	Serous	Primary	3	I	No	NA	P-C	NA	12–24	3
PDTX-EMC002	Serous	Primary	3	III	No	NA	No	NA	>24	5
PDTX-EMC008	Serous	Primary	3	III	No	NA	T-C	Yes	12–24	5
PDTX-EMC053	Serous	Primary	3	III	No	NA	T-C	Yes	12–24	2
PDTX-EMC047	Undiff. carcinoma	Recurrence (abdomen)	3	NA	5FU-Cis	no	No	NA	>24	2
PDTX-EMC022	Uterine mesonephric adenocarcinoma	Primary	3	III	No	NA	T-C; Cis	Yes	>24	5
PDTX-EMC007	Uterine mesonephric adenocarcinoma	Recurrence (vagina)	3	NA	T-C	yes	T-C	No	>24	2
PDTX-EMC024	Uterine mesonephric adenocarcinoma	Metastasis (pelvis)	3	NA	No	NA	T-C; Cis	Yes	>24	8

NA: not applicable; Doc = Docetaxel; Cyclo = cyclophosphamide; T = Taxol; C = Carboplatinum; P = Paclitaxel; D = Doxorubicine; Cis = Cisplatinum; H = Hormone (Aromasin); Ixa = Ixabepilone; 5FU = 5-Fluorouracil.

classified in four different subtypes or clusters: POLE (ultramutated), MSI (microsatellite-instable, hypermutated), copy-number low (endometrioid) and copy-number high (serous-like) [3].

Such analyses also highlighted a high rate of PI3K/AKT pathway mutations in ECs, compared to other tumor types, suggesting it as a potential therapeutic target [4]. PI3K and/or mTOR inhibitors are currently being evaluated in clinical trials, either as single agents or in combination [5–8]. Nevertheless, first reports suggest that, as single agents, they are not as efficacious as hoped [9]. One of the reasons behind the failure of a large number of clinical trials for novel targeted therapies is the lack of robust biomarkers for patient's stratification/inclusion. ECs are not an exception and most of the already completed studies did not stratified patients based on the molecular characterization of their tumors. An additional point to consider is that the preclinical models conventionally used to test novel therapies, although informative about the biology of the tumor, are of poor clinical predictive value.

In the last decade there has been an increasing interest in the implementation of patient-derived models as enhanced preclinical tools. In particular, patient-derived tumor xenograft (PDTX) models, established by implanting surgically removed tumor tissue in immunocompromised mice, are expected to fill the gap between preclinical and clinical research [10]. PDTX models for several cancer types, including ovarian, breast, colorectal and pancreatic cancer, have already been established and showed their ability to reflect the histology and molecular features of the original tumors and predict clinical outcomes in response to both chemo- and targeted therapies [10–12].

Here, we present data about the establishment and molecular characterization of a panel of ECs PDTX. Such a collection, comprising all the main histologic and molecular EC subtypes, represents a valuable translational tool to study endometrial cancer cell biology and response to therapy.

2. Materials and methods

2.1. Patient recruitment and sample collection

In collaboration with the PDTX platform of the KU Leuven (Belgium), PDTX models were established using primary or metastatic endometrial carcinomas from patients undergoing surgery in the University Hospitals

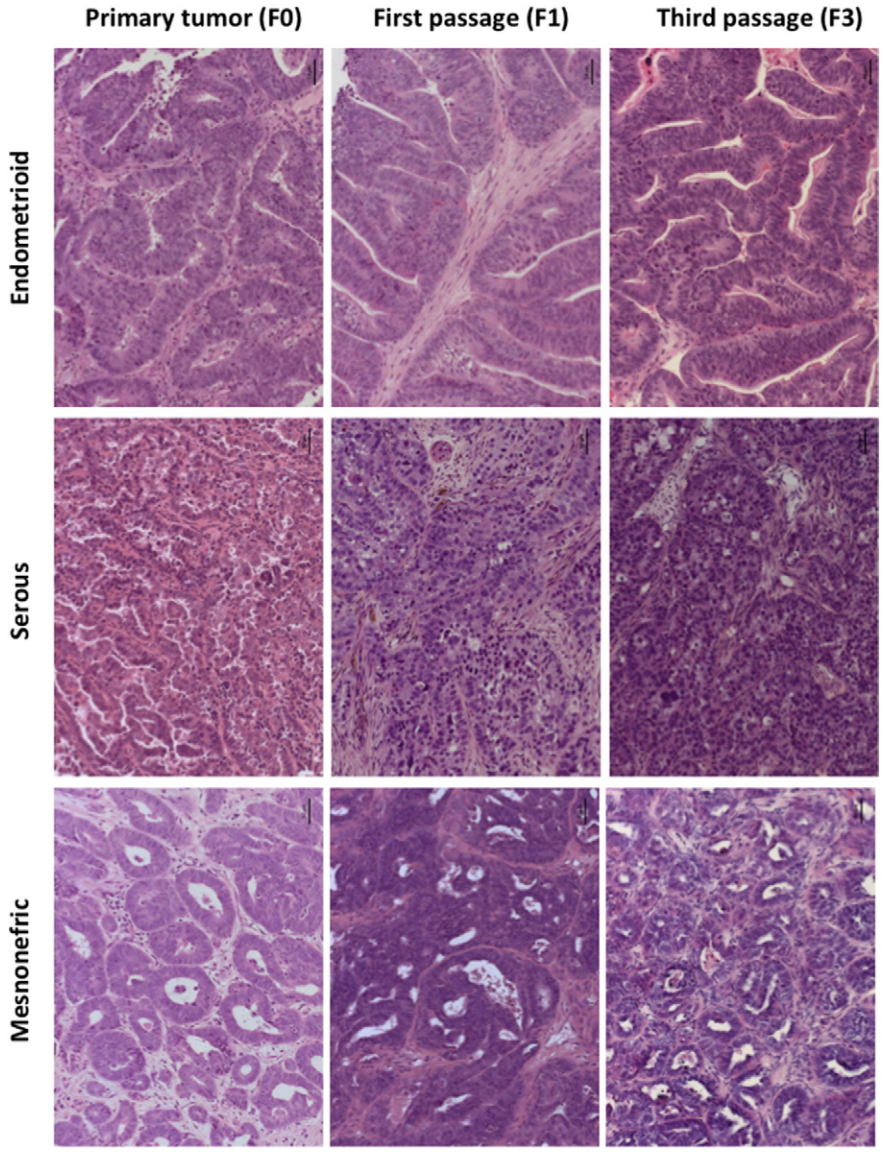

Fig. 1. Histologic overview of endometrial PDTX models. H&E staining of 3 representative models of the different subtypes, an endometrioid, a serous and a mesonefric model. The first (F1) and third (F3) generation xenograft tumors showed over time the same morphology as the primary tumor for all subtypes.

Leuven, Academisch Ziekenhuis Groeninge Kortrijk and Université Catholique de Louvain Saint-Luc Brussels. The study was approved by the local ethical committees in accordance with the principles of the Declaration of Helsinki and all patients gave their written informed consent.

During surgery, fresh tumor tissue was collected in transport medium, [RPMI 1640 medium supplemented with penicillin/streptomycin (100 U/ml; 100 μg/ml), fungizone (1 μg/ml) and gentamicin (50 μg/ml; all from Life Technologies)] and implanted in mice within 4 h. In parallel, primary tumor tissue fragments were also fresh-frozen and formalin-fixed for further analyses.

2.2. Establishment of patient-derived tumor xenografts

Before implantation, tumor tissue was rinsed in PBS (Life Technologies) supplemented with penicillin/streptomycin and fungizone, minced into pieces of 8–10 mm^3 and implanted subcutaneously (s.c.) in both flanks or in the interscapular region of anesthetized 6-weeks-old female immunocompromised Nude mice (Taconic, Denmark) (first generation, F1). When the tumors reached a tumor volume of 1500 mm^3, mice were euthanized, tumors were harvested and general necropsy was performed. Xenograft tumors were immediately fresh-frozen, formalin-fixed or placed in the transport medium for serial transplantation into another set of immunocompromised mice (F2 generation). This process was repeated to produce subsequent generations. The KU Leuven ethical committee approved all animal procedures.

2.3. Histological evaluation of patient-derived tumor xenografts

For all PDTX models, formalin-fixed, paraffin-embedded (FFPE) tissues sections from patient tumor samples and xenografts were stained with hematoxylin and eosin (H&E). Immunohistochemical stainings were performed on deparaffinized FFPE tissue sections using antibodies against estrogen receptor (ER: 1/25; Dako), progesterone receptor (PGR: 1/40; Novocastra), human cytokeratin (CYT: 1/400; Dako), human-mouse vimentin (hu + mo-VIM; 1/1000; Novus Biologicals), human vimentin (hu-VIM: 1/1000; Dako), Mouse-α-Human MutS protein Homolog 1 (MLH1) (1/200; Dako), Mouse-α-Human MutS protein Homolog 2 (MSH2: 1/50; Dako) or Rabbit-α-Human MutS protein Homolog 6 (MHS2: 1/50; Dako). Endogenous peroxidase activity was quenched by incubation with 0.5% hydrogen peroxide in methanol and washed in Tris-buffered saline (TBS). For epitope retrieval, sections were exposed to citrate buffer (pH 6.0) for 1 h at 80 °C (hu + mouse-VIM, hu-VIM), 1 h at 95 °C (MSH6) or for 2 h at 90 °C (PGR). For MHL1 and MSH2 stainings, sections were incubated for 1 h in Tris–HCl buffer (pH 9.0) with 1 mM EDTA at 95 °C and for ER staining incubation of 2 h in Tris–HCl buffer (pH 9.0) with 1 mM EDTA at 90 °C was performed. For CYT staining, sections were enzymatically treated with 0.04% pepsin in 0.01 N HCl for 10 min at 37 °C. After blocking with 2% bovine serum albumin, 2% milk powder and 0.01% Tween in TBS, sections were incubated with the primary antibodies for 2 h (CYT) or overnight (ER, PGR, hu + mouse-VIM, hu-VIM, MLH1, MSH2 and MSH6) in TBS, followed by incubation with the corresponding secondary antibody labeled with horseradish peroxidase for 30 min and antibody binding was

A

MSS	MSI	POLE
PDTX-EMC003	PDTX-EMC001	PDTX-EMC028
PDTX-EMC015	PDTX-EMC016	PDTX-EMC032
PDTX-EMC049	PDTX-EMC034	
	PDTX-EMC040	
	PDTX-EMC042	
	PDTX-EMC044	
	PDTX-EMC046	
	PDTX-EMC056	

B

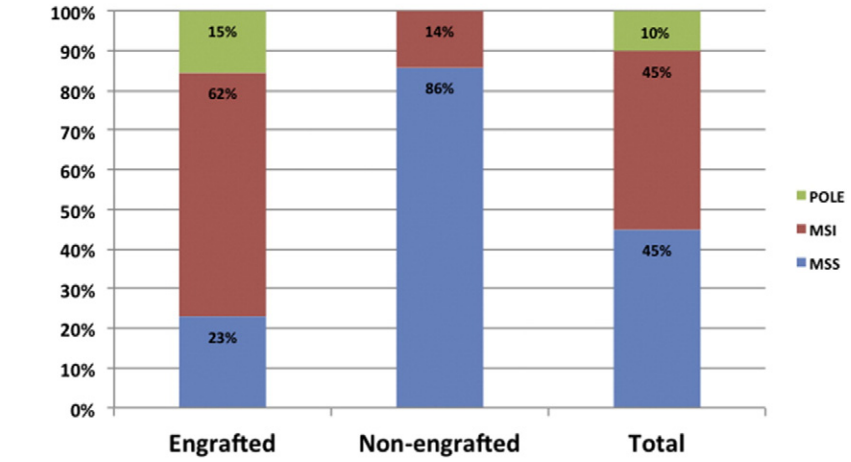

Fig. 2. Frequency of MSI and POLE mutated tumors in endometrioid EC models. A) Status of different successfully engrafted endometrioid EC models. B) Frequency of MSI (red), MSS (bleu) and *POLE*-mutated (green) endometrioid EC models in engrafted and non-engrafted samples. Engrafted models had significantly ($p = 0.028$) more MSI and *POLE*-mutated samples compared to non-engrafted models.

visualized using 3,3-diaminobenzidine chromogen (DAB; Dako). Sections were counterstained with Mayer's Hematoxylin.

2.4. Somatic single nucleotide variant detection by Whole Exome Sequencing (WES)

DNA was extracted from primary tumor samples and the corresponding xenograft (F3 generation) using DNeasy Blood and Tissue Kit (Qiagen). Presence of tumor tissue was checked with H&E slides. Micro-satellite instability (MSI) was checked as previously described by Zhao et al. [13]. *POLE* mutations were sequenced by Sanger Sequencing of exons 9 and 13 [14].

Whole-exome sequencing was performed, as described previously [13,15]. DNA libraries for WES were prepared using the KAPA DNA Library Preparation Kit (Illumina). After library preparation, exonic fragments were captured with SeqCap EZ Human Exome Library (Roche). These libraries were clustered on an Illumina V3 flowcell for subsequent 2 × 100 base pair pair-end sequencing on a HiSeq2000 with an average coverage of 30× for germline, patient tumor and xenograft samples. Raw sequencing reads were mapped to the human reference genome (NCBI37/hg19) using Burrows-Wheeler Aligner (BWA) and processed and sorted with SAM tools. Duplicate reads were removed using Picard tools. Base recalibration, local realignment around insertions and deletions and single nucleotide variant calling were performed using the Genome Analysis Tool Kit. To distinguish patient-specific mutations from mouse DNA in the xenograft, all reads were mapped to both human (NCBI37/hg19) and mouse (GRCm38/mm^{10}) reference genome. Reads that mapped unique to human genome were selected and used for further analysis. Common variants (Major Allelic Frequency >1%) were filtered out using the following databases: dbSNP version 132, 1000 Genomes Project, Axiom Genotype Data Set and the Complete Genomics diversity panel (46 Hapmap individuals). Exonic non-synonymous mutations were selected for downstream analysis with a coverage less than 5× in the germline DNA and higher then 10× in the primary tumor or xenograft. The cancer consensus genes described by COSMIC [16] were used to compare between the mutation profiles of primary and corresponding xenograft tumors.

2.5. Copy number alteration detection by whole-genome low-coverage (shallow) sequencing

DNA libraries for sequencing were prepared using KAPA DNA Library Preparation Kit (Illumina). After library preparation, samples were sequenced at low coverage on a HiSeq2000 (Illumina) using a V3 flowcell generating 1 × 50 bp reads. Raw sequencing reads were mapped to the human reference genome (NCBI37/hg19) using Burrows-Wheeler Aligner (BWA), revealing on average 12,124,835 mapped reads. Copy-number alterations were identified by QDNAseq v. 1.0.5 [17] by binning the reads in 100 kb windows. Bins in problematic regions were blacklisted, read counts were corrected for GC-content and mappability using LOESS regression. Read counts were normalized by the median and outliers were smoothed. Segmentation of the bin values was performed by ASCAT v. 2.0.7 [18]. When comparing the copy number alterations between primary tumor and xenograft, each region with an absolute difference in copy number of >0.5 was assumed to be different between primary tumor and xenograft

2.6. Evaluation of the efficacy of NVP-BEZ235 and AZD6244 in the established PDX models

The efficacy of treatment with NVP-BEZ235 (dual pan-PI3K/mTOR inhibitor) and AZD6244 (MEK inhibitor) (Selleck Chemicals) on tumor growth of mice bearing tumors with *PTEN*, *PIK3CA* and *KRAS* mutations (PDTX-EMC003 model) was evaluated. Tumor tissues of 9 mm^3 were s.c. implanted in the flank of NRMI nude mice of 6 weeks old. Mice were treated as previously described [19]. Briefly, when tumors reached a volume of ~150 mm^3 mice were randomly distributed into five groups (5 mice/group) and treated with either vehicle (10% NMP with 90% PEG) (Sigma Aldrich), NVP-BEZ235 (40 mg/kg, daily, p.o.), AZD6244 (25 mg/kg, daily, p.o.), the combination of NVP-BEZ235 (40 mg/kg) with AZD6244 (25 mg/kg) or carboplatin (50 mg/kg, 1×/week, i.p.). For oral administration, NVP-BEZ235 and AZD6244 were dissolved 10% NMP with 90% PEG. Control animals received the equivalent volume of vehicle (placebo group). All mice were treated for four weeks. Mice were sacrificed 1 h after last treatment administration. Xenografts were harvested, weighed and processed for further analyses (fresh-frozen and formalin-fixed).

All mice were weighed at regular intervals and screened for adverse effects. Tumor size was measured 2×/week with a caliper and tumor volume was calculated using the following formula: L × W^2/2, with L = tumor length; W = tumor width.

2.7. Western blotting

Total protein lysates were prepared from post-treatment fresh-frozen tumor fragments using the mammalian cell lysis MCL1 kit (Sigma Aldrich) according to the manufacturer's instructions. Total protein concentration was determined with the Pierce BCA protein assay kit (Thermo Scientific). An equal amount of proteins (30 μg) was resolved in sodium dodecyl sulfate sample buffer, subjected to any kD Mini Protein TGX gels (Bio-Rad) and transferred to a polyvinylidene difluoride membrane (Bio-Rad). Non-specific binding was blocked by

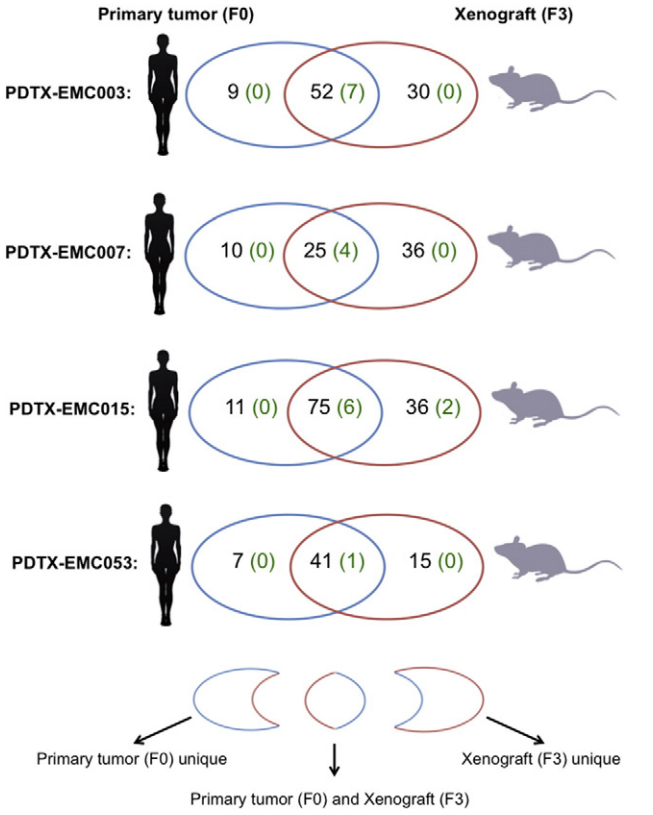

Fig. 3. Non-synonymous mutations in primary tumor and xenograft for PDTX-EMC003, PDTX-EMC007, PDTX-EMC015 and PDTX-EMC053. Blue circles indicate mutations from primary tumor, red indicate mutations from the xenograft. Common mutations between primary tumor and xenograft are found in the center. Mutations found to be cancer genes according to COSMIC are in green.

incubation of the membrane in blocking buffer (5% non-fat dry milk with 0.05% Tween in TBS). Next, membranes were incubated overnight at 4 °C with the following primary antibodies (Cell Signaling Technologies): AKT, p-AKT$^{(Ser473)}$, S6, p-S6$^{(Ser235/Ser236)}$, ERK1/2, p-ERK1/2$^{(Thr202/Tyr204)}$ (all 1/1000), and beta-actin (1/2500) as a loading control, after which membranes were incubated with rabbit or mouse horseradish peroxidase-conjugated secondary antibodies (Bio-Rad). All blots were developed by enhanced chemiluminescence and bands were visualized using the FUJI mini-LAS 4000-plus imaging system (GE Healthcare).

2.8. Statistics

One-way ANOVA for repeated measurements followed by a Tukey's multiple comparison test was performed to assess differences in therapy response over time between treatment groups. One-way

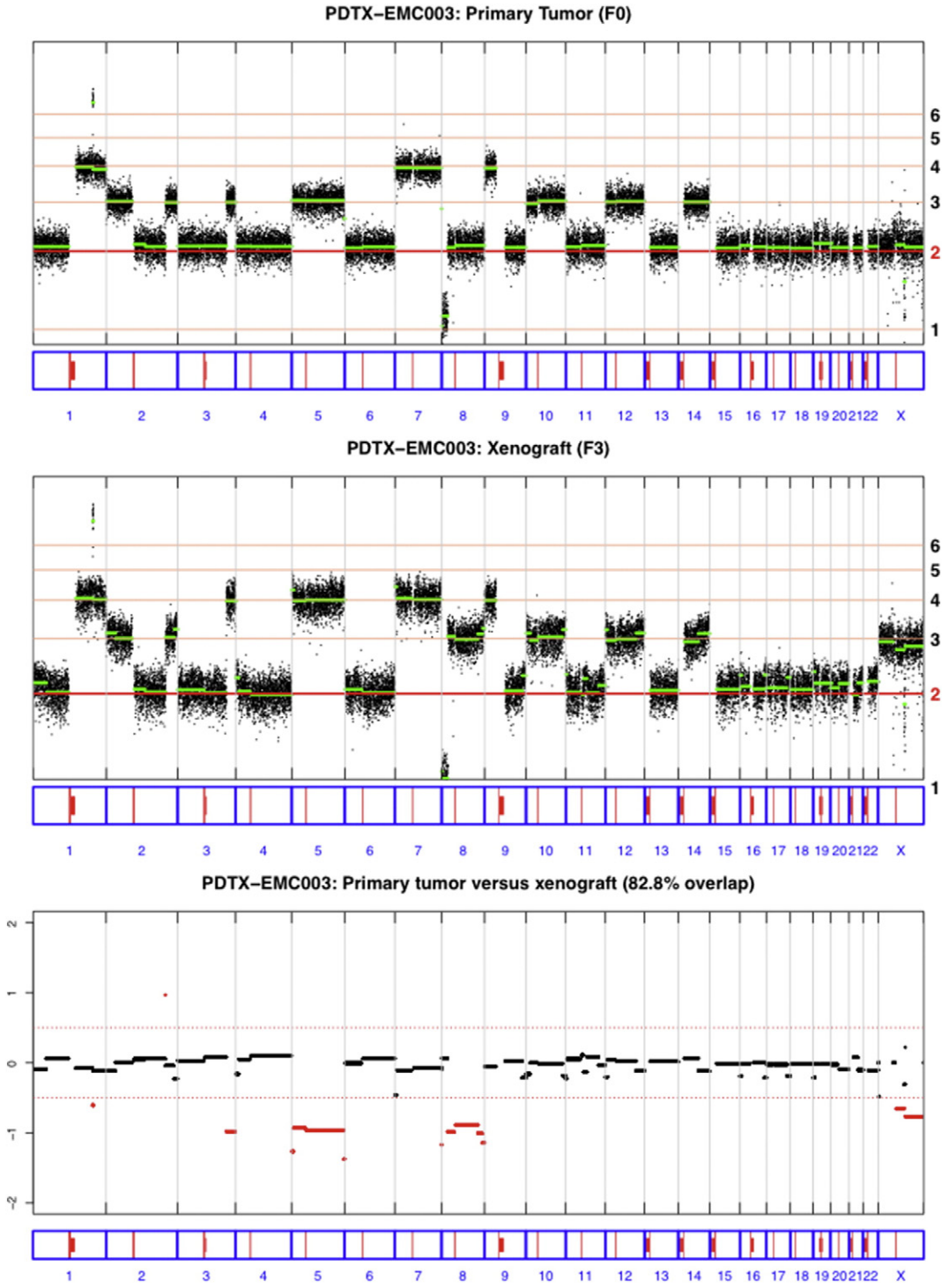

Fig. 4. Copy number alterations in PDTX-EMC003 obtained from whole genome low coverage sequencing. Centromeric regions are indicated as large red boxes below the figures. Acrocentric chromosomes and heterechromatin (pericentric or telomeric) regions as small red boxes. Primary tumor and xenograft were compared by calculating the difference in copy number of each fragment between primary tumor and xenograft. Fragments with an absolute difference of more than 0.5 are indicated in red. Threshold values −0.5 and +0.5 indicated as red dotted lines.

ANOVA followed by Tukey's multiple comparison test was performed to assess differences in tumor weight between treatment groups. Statistical analyses were performed using Graphpad Prism 5 software. Results are shown as mean ± standard error of mean (SEM). $p < 0.05$ was considered as statistically significant.

3. Results

3.1. Establishment of a panel of endometrial cancer patient-derived tumor xenografts

We transplanted a total of 40 fresh primary, metastatic and/or recurrent EC samples, obtained immediately after surgery, into immunocompromised mice and PDTXs were successfully engrafted from 24 of them. Of these, 17 xenografts have been propagated beyond an F3 generation, while 7 tumors are still growing in F2. Among the 40 models, 16 models did not grow in F1. Taken together, a success rate of 60% was reached when both F3 tumors and growing tumors were considered as successfully engrafted. We validated extensively 17 EC PDTX models, since of these tumors the F3 xenografts were available for histologic and genomic analysis. An overview of the successfully growing PDTX models and their clinical characteristics of the original patients is represented in Table 1.

3.2. EC patient-derived tumor xenografts maintained the histologic characteristics of the corresponding patient tumor

To histologically validate the established PDTX models, we compared their general morphology, hormone receptor (ER, PGR) status and CYT expression to the one of the corresponding primary tumor. In all the models, irrespectively of their histological classification, the tissue architecture and the epithelial compartment of the original tumor, as shown by H&E and CYT staining, was preserved in the corresponding F1 and F3 PDTXs (Fig. 1 and S1, respectively). In general, we observed similarities in ER and PGR stainings between patient and xenograft tumors (Fig. S1), although in general PGR expression seems to be reduced in the xenografts.

3.3. In EC patient-derived tumor xenografts the human stromal component is replaced by a reduced amount of murine stroma

To characterize the stroma in the PDTX tumors, we stained tumor sections for vimentin, using two different antibodies: one specific for human vimentin (hu-VIM) and a second one binding both human and mouse vimentin (hu + mo-VIM). In all patient tumors, the stroma stained positive for hu-VIM, but the staining was negative in the PDTXs, indicating that the human-derived stroma was lost after tumor

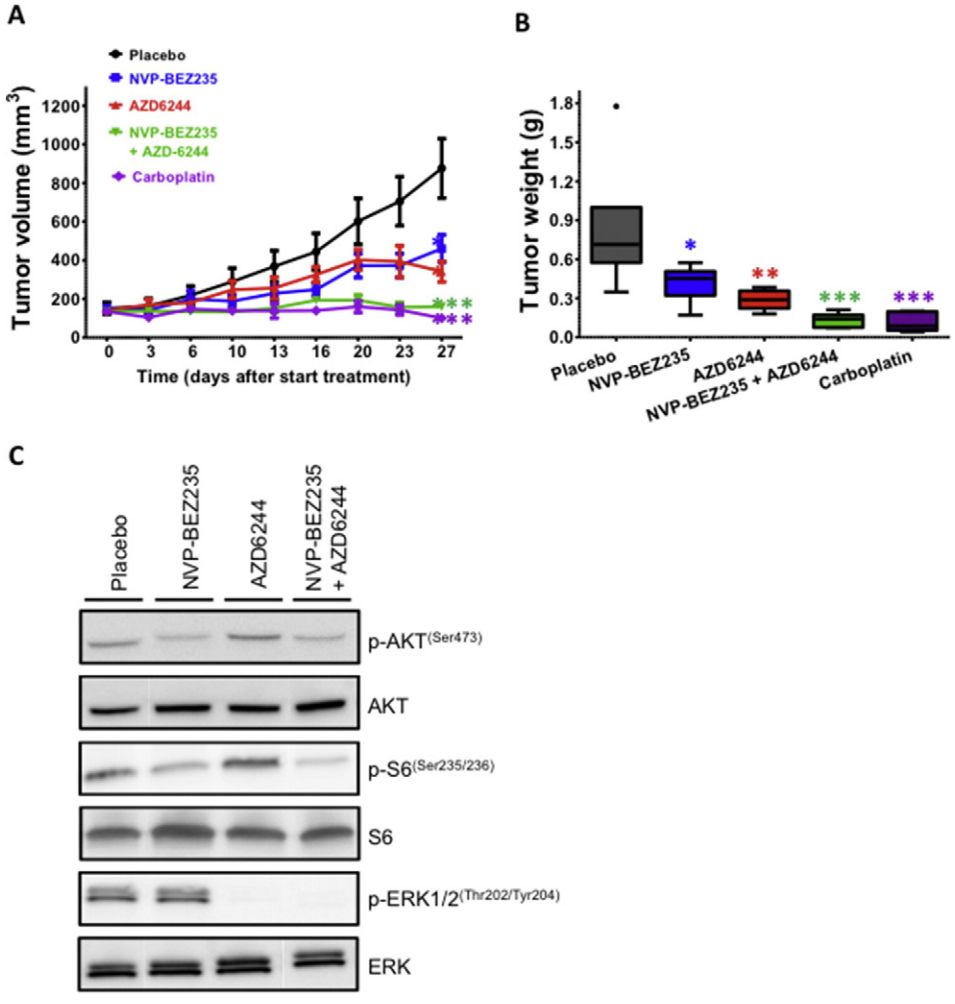

Fig. 5. NVP-BEZ235 and AZD6244 reduce tumor growth in PDTX model harboring a *PTEN*, *PIK3CA* and *KRAS* mutation. A) Tumor-bearing nude mice were treated with either NVP-BEZ235 (40 mg/kg, daily, p.o.) or AZD6244 (25 mg/kg, daily, p.o.) or both (n = 5 mice/group) for four weeks. Single treatment of NVP-BEZ235 or AZD6244 showed tumor growth suppression. Combination treatment showed stabilization of tumor growth. One-way ANOVA for repeated measurements followed by a Tukey's multiple comparison test. B) Wet tumor weight showed a significant difference in tumor weight compared to placebo group. One-way ANOVA followed by Tukey's multiple comparison test. C) Phosphorylation of AKT and S6 is reduced for tumors of mice treated with NVP-BEZ235. In addition, AZD6244 induced reduction of p-ERK1/2 expression. Combination treatment showed reduction of phosphorylation of AKT, S6, and ERK1/2. Results are shown as mean ± SEM. $^{*}p < 0.05$, $^{**}p < 0.01$, $^{***}p < 0.001$, compared with placebo group.

engraftment in mice (Fig. S2). The human- and mouse-specific antibody against vimentin was strongly positive for xenograft stroma, confirming that, as already reported for other PDTX models [20], the human stroma is replaced by a reduced amount of murine stroma after engraftment.

3.4. Engrafted endometrioid EC PDTX samples are enriched with MSI and POLE mutated samples

MSI and *POLE* mutations are common in endometrioid ECs (33–40% and 7% of the cases, respectively) and result in a higher mutation frequency [3]. We checked all the engrafted and non-engrafted endometrioid samples for MSI and *POLE* mutations (Fig. 2) and, comparing them, we observed a significant enrichment of MSI and *POLE* mutated tumors in the engrafted samples (Fisher's exact test; $p = 0.028$). The MSI status was also confirmed by immunohistochemical staining, since MSI tumors are associated with a decreased expression of nuclear MLH1, MSH2 or MSH6 [13]. All primary and correlated xenograft tumors were positive for MSH2 and MHS6. In contrast, MSS tumors expressed MLH1, whereas MSI tumors were negative for MLH1 (data not shown).

3.5. Genetic analysis on patient-derived tumor xenograft showed high similarity with patient tumors

Next, we performed WES on four models reflecting the different more common and relevant subtypes in EC, *i.e.* two endometrioid, one mesonephric and one serous EC. Among the endometrioid EC models, we selected two models (grade 1 and grade 3, respectively) without MSI or *POLE* mutations. We found an average of 57 (range 35–86) non-silent mutations in the primary human tumors and 77 of them (range 56–111) in the xenografts (Fig. 3). The majority of such mutations were common between primary tumor and xenograft (55%), while a minor fraction was unique either for the primary tumor (11%) or for the xenograft (34%). Looking specifically at the cancer consensus genes from COSMIC, we observed that most of the mutations were common between primary tumor and xenograft (Table S1). Next, we validated mutations unique for primary tumor and xenograft with ultra-deep targeted resequencing with a coverage > 500×. Among the 9 validated mutations, 4 were found to be false positives, 3 were present both in primary tumor and xenograft, while only 2 mutations arose during engraftment (Table S2). The latter were both found in PDTX-EMC0015, one mutation in *THRAP3* was detected in a F3 generation and one mutation in *PDE4DIP* was detected in a F1 and F3 generation.

The copy number profiles generated using low-coverage whole-genome sequencing for both the primary tumor and xenograft from PDTX-EMC003 are shown in Fig. 4. Copy number profiles from the other models are shown in Figs. S3–S5. On average, 90% (range 83%–100%) of the genome had the same copy number between primary tumor and xenograft. The regions with deletions or amplifications were thus very well maintained during engraftment, even with the same copy number and breakpoints for each region. Remarkably, this was also observed in the serous subtype (PDTX-EMC053), while serous EC are known to have a very high frequency of copy number alterations [3].

3.6. Endometrial patient-derived tumor xenograft model, with PTEN, PIK3CA and KRAS mutations, is sensitive to combined PI3K/mTOR and MEK inhibition

As a proof of concept, the efficacy of PI3K/mTOR and MEK inhibitors on *in vivo* tumor growth was evaluated in our PDTX-EMC003 PDTX model, a high grade recurrent endometrioid carcinoma carrying *PTEN*, *PIK3CA* and *KRAS* mutations (Table S1). To this purpose, NVP-BEZ235 (dual pan-PI3K/mTOR inhibitor) and AZD6244 (MEK1/2 inhibitor) were selected. In this model, treatment with either NVP-BEZ235 or AZD6244 significantly slowed-down tumor growth as compared to the placebo group. However, when treatment with NVP-BEZ235 and AZD6244 was combined, tumor growth curve results in stable disease (SD), as also observed for Carboplatin treatment (Fig. 5A), and confirmed by wet tumor weight analysis at sacrifice (Fig. 5B). In these treated xenograft tumors, we also evaluated the phosphorylation levels of the targeted molecules and observed that, as expected, NVP-BEZ235 reduced p-AKT and p-S6 expression. In AZD6244-treated tumors p-ERK1/2 levels were markedly reduced. When both treatments were combined, phosphorylation of AKT, S6 and ERK1/2 was reduced (Fig. 5C), confirming the on-target effect of the drugs.

4. Discussion

Patient derived tumor xenograft models have been established and characterized for different types of cancers, including colorectal [21], lung [22], pancreatic [23], breast [24] and ovarian carcinomas [11,12,25]. Used as a complementary tool with the commercially available immortalized cell lines, they showed high potential for preclinical studies because of their ability to recapitulate the clinico-pathological features of the human original tumors. Endometrial carcinomas are the most frequent gynecological malignancies and treatment options are still limited for advanced and recurrent diseases.

Here, we described the establishment of a panel of 24 PDTX Endometrial Cancer models, comprising all the most relevant histological subtypes. Importantly, the models closely resemble the histological architecture of the original tumor tissues. As already shown for other types of PDTX, once engrafted in mice, the human stromal compartment of the tumors is replaced by a reduced amount of murine stroma. Although this might represent a caveat for the use of the models for testing stromal-directed therapies (such as antiangiogenic agents), it has been recently showed that in colorectal cancer PDTX such phenomenon could be exploited to dissect the role of the epithelial and stromal compartment in tumor development [26].

Notably, we demonstrated that PDTX models can be successfully established from both type I and type II endometrial carcinomas, with an overall engraftment rate of 60%. MSI and *POLE* mutations are a phenomenon that occurs in about 33–40% and 7% of all endometrioid EC, respectively [3]. Of the analyzed PDTX models, 62% were MSI and 15% *POLE* mutated. MSI and *POLE* mutated tumors can be resistant to targeted therapies, because they acquire secondary mutations in genes that activate alternative or downstream signaling pathways. We observed a strong enrichment of MSI xenografts, suggesting a growth advantage for such hypermutated tumors in mice, indicating the importance to test endometrioid EC PDTX models for MSI and *POLE* mutations, especially when these models are used for the evaluation of targeted therapies. To characterize at the molecular level the genomic landscape of our PDTXs, we performed Whole Exome Sequencing and copy number variation analyses on 4 models, representative of each relevant EC subtypes: 1 low grade and 1 high grade endometrioid, 1 serous and 1 mesonephric. With regard to non-synonymous mutations, most mutations were common between primary tumor and xenograft and a small fraction of the mutations were unique for the primary tumor and xenograft. Of note, we observed mutations in some of the most frequently mutated genes in EC, such as *PIK3CA*, *PTEN*, *ARID1A* and *KRAS*. Importantly, all but two mutations in cancer consensus genes were retained between patient tumors and their corresponding xenografts, meaning most of the primary or xenograft unique mutations are just passenger mutations. In addition, the copy number profile of the different models was very stable during engraftment, with an average similarity of 90%.

Clinically relevant models, in addition to mirror the histological and genomic features of the tumors in the patients, should also be of predictive value about responses to standard and/or novel therapeutic regimens. In particular, there is urgent need for preclinical models with strong translational potential to test the efficacy of targeted therapies in EC patients with advanced, metastatic and recurrent diseases. PI3K/AKT/PTEN/mTOR pathway is one of the most frequently dysregulated

pathways in ECs and we characterized one of our PDTX models, PDTX-EMC003 (recurrent endometrioid carcinoma carrying *PTEN*, *PIK3CA* and *KRAS* mutations, established from a patient at end-stage of disease), for the response to NVP-BEZ235 (dual pan-PI3K/mTOR inhibitor), AZD6244 (MEK1/2 inhibitor) and the combination of the two, since PI3K/AKT/mTOR and Ras/Raf/MEK pathways can regulate each other by cross-inhibition and cross-activation [27]. We observed that single treatments with the targeted agents were able to just slow-down the growth of the tumors, while the combination resulted in stable disease, as also observed after Carboplatinum administration. Since protein expression analyses showed the on-target effect of both drugs but only stable disease was achieved, this model might represent an optimal candidate to study the molecular mechanisms engaged by the tumor to resist to both chemo- and targeted therapies.

Here, we reported about the establishment of a panel of PDTX models comprising the major histological and molecular subtypes of endometrial cancer. Collectively, our data showed that such models closely resemble the original human tumors in the patients in term of tissue architecture and genomic features. A pilot treatment experiment with targeted therapies against specific mutations in one of the model also suggests that clinically annotated PDTXs might be of strong potential for both fundamental and translational studies in ECs.

Supplementary data to this article can be found online at http://dx.doi.org/10.1016/j.ygyno.2015.07.104.

Conflict of interest statement

The authors have no financial relationship or conflicts of interest to report.

Acknowledgments

This study was supported by a grant of the Belgian Foundation against Cancer (Grant No. KPC_29_005). In addition, this work was funded by the Anticancer Fund through the Verelst Uterine Cancer Fund Leuven. for scientific and financial support.

References

[1] R. Siegel, J. Ma, Z. Zou, A. Jemal, Cancer statistics, 2014, CA Cancer J. Clin. 64 (2014) 9–29.
[2] F. Amant, P. Moerman, P. Neven, D. Timmerman, E. Van Limbergen, I. Vergote, Endometrial cancer, Lancet 366 (2005) 491–505.
[3] TCGA, Integrated genomic characterization of endometrial carcinoma, Nature 497 (2013) 67–73.
[4] A.P. Myers, New strategies in endometrial cancer: targeting the PI3K/mTOR pathway—the devil is in the details, Clin. Cancer Res. 19 (2013) 5264–5274.
[5] R.A. Goodwin, R. Jamal, D. Tu, W. Walsh, J. Dancey, A.M. Oza, et al., Clinical and toxicity predictors of response and progression to temsirolimus in women with recurrent or metastatic endometrial cancer, Gynecol. Oncol. 131 (2013) 315–320.
[6] A.M. Oza, L. Elit, M.S. Tsao, S. Kamel-Reid, J. Biagi, D.M. Provencher, et al., Phase II study of temsirolimus in women with recurrent or metastatic endometrial cancer: a trial of the NCIC Clinical Trials Group, J. Clin. Oncol. 29 (2011) 3278–3285.
[7] F.I. Raynaud, S. Eccles, P.A. Clarke, A. Hayes, B. Nutley, S. Alix, et al., Pharmacologic characterization of a potent inhibitor of class I phosphatidylinositide 3-kinases, Cancer Res. 67 (2007) 5840–5850.
[8] B.M. Slomovitz, K.H. Lu, T. Johnston, R.L. Coleman, M. Munsell, R.R. Broaddus, et al., A phase 2 study of the oral mammalian target of rapamycin inhibitor, everolimus, in patients with recurrent endometrial carcinoma, Cancer 116 (2010) 5415–5419.
[9] H.B. Salvesen, I.S. Haldorsen, J. Trovik, Markers for individualised therapy in endometrial carcinoma, Lancet Oncol. 13 (2012) e353–e361.
[10] M. Hidalgo, F. Amant, A.V. Biankin, E. Budinska, A.T. Byrne, C. Caldas, et al., Patient-derived xenograft models: an emerging platform for translational cancer research, Cancer Discov. 4 (2014) 998–1013.
[11] Z.C. Dobbin, A.A. Katre, A.D. Steg, B.K. Erickson, M.M. Shah, R.D. Alvarez, et al., Using heterogeneity of the patient-derived xenograft model to identify the chemoresistant population in ovarian cancer, Oncotarget 5 (2014) 8750–8764.
[12] S.J. Weroha, M.A. Becker, S. Enderica-Gonzalez, S.C. Harrington, A.L. Oberg, M.J. Maurer, et al., Tumorgrafts as in vivo surrogates for women with ovarian cancer, Clin. Cancer Res. 20 (2014) 1288–1297.
[13] H. Zhao, B. Thienpont, B.T. Yesilyurt, M. Moisse, J. Reumers, L. Coenegrachts, et al., Mismatch repair deficiency endows tumors with a unique mutation signature and sensitivity to DNA double-strand breaks, eLife 3 (2014) e02725.
[14] D.N. Church, E. Stelloo, R.A. Nout, N. Valtcheva, J. Depreeuw, N. ter Haar, et al., Prognostic significance of POLE proofreading mutations in endometrial cancer, J. Natl. Cancer Inst. 107 (2015) 402.
[15] J. Reumers, P. De Rijk, H. Zhao, A. Liekens, D. Smeets, J. Cleary, et al., Optimized filtering reduces the error rate in detecting genomic variants by short-read sequencing, Nat. Biotechnol. 30 (2012) 61–68.
[16] P.A. Futreal, L. Coin, M. Marshall, T. Down, T. Hubbard, R. Wooster, et al., A census of human cancer genes, Nat. Rev. Cancer 4 (2004) 177–183.
[17] I. Scheinin, D. Sie, H. Bengtsson, M.A. van de Wiel, A.B. Olshen, H.F. van Thuijl, et al., DNA copy number analysis of fresh and formalin-fixed specimens by shallow whole-genome sequencing with identification and exclusion of problematic regions in the genome assembly, Genome Res. 24 (2014) 2022–2032.
[18] P. Van Loo, S.H. Nordgard, O.C. Lingjaerde, H.G. Russnes, I.H. Rye, W. Sun, et al., Allele-specific copy number analysis of tumors, Proc. Natl. Acad. Sci. U. S. A. 107 (2010) 16910–16915.
[19] S. Schrauwen, J. Depreeuw, L. Coenegrachts, E. Hermans, D. Lambrechts, F. Amant, Dual blockade of PI3K/AKT/mTOR (NVP-BEZ235) and Ras/Raf/MEK (AZD6244) pathways synergistically inhibit growth of primary endometrioid endometrial carcinoma cultures, whereas NVP-BEZ235 reduces tumor growth in the corresponding xenograft models, Gynecol. Oncol. 138 (2015) 165–173.
[20] Y.S. DeRose, G. Wang, Y.C. Lin, P.S. Bernard, S.S. Buys, M.T. Ebbert, et al., Tumor grafts derived from women with breast cancer authentically reflect tumor pathology, growth, metastasis and disease outcomes, Nat. Med. 17 (2011) 1514–1520.
[21] S. Julien, A. Merino-Trigo, L. Lacroix, M. Pocard, D. Goere, P. Mariani, et al., Characterization of a large panel of patient-derived tumor xenografts representing the clinical heterogeneity of human colorectal cancer, Clin. Cancer Res. 18 (2012) 5314–5328.
[22] X.C. Zhang, J. Zhang, M. Li, X.S. Huang, X.N. Yang, W.Z. Zhong, et al., Establishment of patient-derived non-small cell lung cancer xenograft models with genetic aberrations within EGFR, KRAS and FGFR1: useful tools for preclinical studies of targeted therapies, J. Transl. Med. 11 (2013) 168.
[23] M. Mattie, A. Christensen, M.S. Chang, W. Yeh, S. Said, Y. Shostak, et al., Molecular characterization of patient-derived human pancreatic tumor xenograft models for preclinical and translational development of cancer therapeutics, Neoplasia 15 (2013) 1138–1150.
[24] E. Marangoni, A. Vincent-Salomon, N. Auger, A. Degeorges, F. Assayag, P. de Cremoux, et al., A new model of patient tumor-derived breast cancer xenografts for preclinical assays, Clin. Cancer Res. 13 (2007) 3989–3998.
[25] F. Ricci, F. Bizzaro, M. Cesca, F. Guffanti, M. Ganzinelli, A. Decio, et al., Patient-derived ovarian tumor xenografts recapitulate human clinicopathology and genetic alterations, Cancer Res. 74 (2014) 6980–6990.
[26] C. Isella, A. Terrasi, S.E. Bellomo, C. Petti, G. Galatola, A. Muratore, et al., Stromal contribution to the colorectal cancer transcriptome, Nat. Genet. 47 (2015) 312–319.
[27] M.C. Mendoza, E.E. Er, J. Blenis, The Ras-ERK and PI3K-mTOR pathways: cross-talk and compensation, Trends Biochem. Sci. 36 (2011) 320–328.